Discrete Non-Orthogonal Shell Model: from mid-mass to heavy deformed nuclei

Duy-Duc Dao, F. Nowacki

(IPHC-Strasbourg)

14th International Spring Seminar on Nuclear Physics

Ischia, May 19-23th, 2025

CNRS IN2P3 Les deux infinis — IPHC Institut Pluridisciplinaire Hubert CURIEN Strasbourg — Université de Strasbourg

Outline

1. Generalities of the Shell Model framework

2. Discrete Non-Orthogonal Shell Model (DNO-SM)

   - Exact eigenstates of shell-model Hamiltonians with symmetry-projected Slater determinants
   - Illustrations from light- to mid-mass deformed nuclei

3. Applications to superheavy nuclei

4. Conclusions

SM-CI approaches through the nuclear chart

Fundamental interactions and collectives excitations

- Deformation, Superdeformation, Dipole/M1 resonances
- Superfluidity, Symmetries
- Isospin symmetry breaking

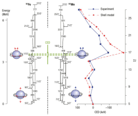

Weak processes

- β decay $\Longleftrightarrow$ fundamental interactions
- $\beta\beta$ decay $\Longleftrightarrow$ nature of neutrinos

$$[T^{0\nu}_{1/2}(0^+ \to 0^+)]^{-1} = G_{0\nu}\,|M^{0\nu}|^2\,\langle m_\nu\rangle^2$$

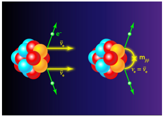

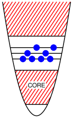

- $\mathcal{H}_{\text{exact}}\Psi_{\text{exact}} = E\Psi_{\text{exact}}$

$\Updownarrow$

- $\mathcal{H}_{\text{eff}}\Psi_{\text{eff}} = E\Psi_{\text{eff}}$

Treat Many-Body problem
Treat Effective Interaction

Nuclear structure far from stability

- New magic numbers
- Vanishing of shell closures

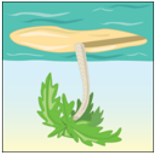

Astrophysics and nucleosynthesis

- rp process
- r process

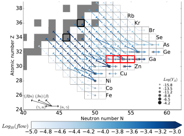

Monopole-corrected effective interactions

△ V-low k derived from NN interactions

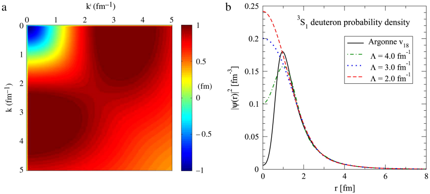

(S.K. Bogner, R.J. Furnstahl, A. Schwenk, Prog. Part. Nucl. Phys. **65**, 1 (2010) 94-147)

△ Valence-space MBPT renormalization

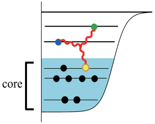

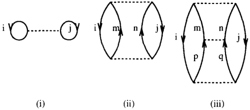

(H.-W. Hammer *et al.* Rev. Mod. Phys. **85**, 197 (2013))

(M. Hjorth-Jensen *et al.* Phys. Rep. **261** (1995) 125-270)

△ Multipole decomposition

$$H = H_{monopole} + H_{multipole}$$

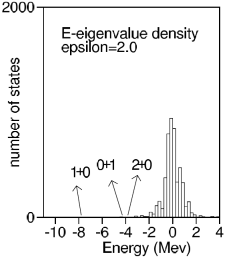

A. Zuker, physics

$H_{monopole}$: spherical mean-field

☞responsible for the global saturation properties and for the evolution of the spherical single particle levels.

$H_{multipole}$: correlator

☞ pairing, quadrupole, octupole...

Monopole-corrected effective interactions

△ V-low k derived from NN interactions

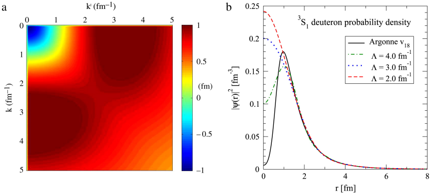

(S.K. Bogner, R.J. Furnstahl, A. Schwenk, Prog. Part. Nucl. Phys. **65**, 1 (2010) 94-147)

△ Valence-space MBPT renormalization

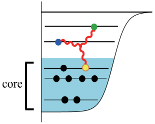

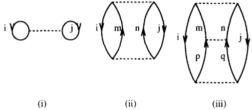

(H.-W. Hammer *et al.* Rev. Mod. Phys. **85**, 197 (2013)) (M. Hjorth-Jensen *et al.* Phys. Rep. **261** (1995) 125-270)

△ Multipole decomposition

$$H = H_{monopole} + H_{multipole}$$

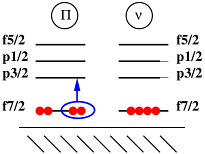

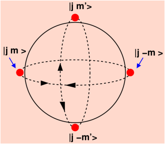

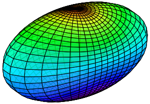

$H_{monopole}$: spherical mean-field

☞responsible for the global saturation properties and for the evolution of the spherical single particle levels.

$H_{multipole}$: correlator

☞ pairing, quadrupole, octupole...

Diagonalization versus Variational Methods

Shell Model Exact Diagonalization

- Exponential growth of basis dimensions :

$$D \sim \begin{pmatrix} d_\pi \\ p \end{pmatrix} \cdot \begin{pmatrix} d_\nu \\ n \end{pmatrix}$$

In *pf* shell :

^{48}Cr **1,963,461**

^{56}Ni **1,087,455,228**

In *pf-sdg* space :

^{78}Ni **210,046,691,518**

ANTOINE CODE (1989)

- Actual limits in giant diagonalizations :
  $\sim 10^{12}$, $\sim 10^{15}$ $\neq 0$ matrix elements
- Some of the largest diagonalizations ever are performed in Strasbourg with relatively modest computationnal ressources :
  E. Caurier et al., Rev. Mod. Phys. 77 (2005) 427

• m-scheme	ANTOINE code
	BIGSTICK
	KSHELL
• coupled scheme	NATHAN code

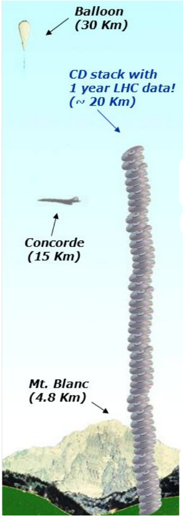

Variational Approximation

$$\mathcal{H}_{\text{eff}}|\Psi_\alpha^{JM}\rangle = E_\alpha^{(J)}|\Psi_\alpha^{JM}\rangle \rightarrow \delta \frac{\langle\Psi_\alpha^{JM}|\mathcal{H}_{\text{eff}}|\Psi_\alpha^{JM}\rangle}{\langle\Psi_\alpha^{JM}|\Psi_\alpha^{JM}\rangle} = 0$$

- **Mixing of shapes:**

$|\Psi_{\text{eff}}\rangle =$ 

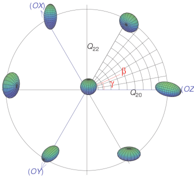

- **Restoration of the rotational symmetry**
- **Degree of freedom**
  - Multipole: β, γ, Q_{30}, ...
  - Cranking: J_x, J_z
  - Pairing constraints
  - Variation-After-Projection
- **Different implementations**

• MCSM	Tokyo group
• DNO-SM	Strasbourg group
• Taurus code	Madrid group

Discrete Non-Orthogonal Shell Model (DNO-SM)

- Broeckhove-Deumens Theorem: Z. Phys. A**292**, 243 (1979)

  Given a separable Hilbert space $\mathscr{H}$ spanned by a continuous family of states $\Gamma = \{\psi(\alpha)|\alpha \in \mathbb{R}\}$, there exists a countable subset $\Gamma_0 = \{\phi(\alpha_i)|i \in \mathbb{N}\} \subset \Gamma$ with the property $\mathscr{H} = \overline{\mathrm{span}\Gamma_0}$, i.e. Γ_0 is a skew or non-orthogonal basis in $\mathscr{H}$.

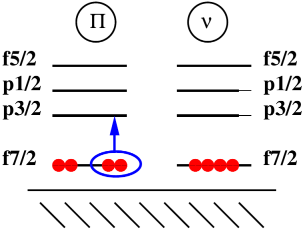

$$\psi = c_1\phi_1 + c_2\phi_2 + \cdots + c_3\phi_3 + \ldots$$

Finite Countable Set of Non-Orthogonal Slater Determinants spanning the full shell-model space.

◇ Several questions

- Ground state underbinding energy?
- Incorporation of correlations?
- Numerical proof of Broeckhove-Deumens Theorem?

PFSDG-U effective interaction

^{78}Ni	DNO-SM(β,γ)	SM (10p-10h)
dimension	81	$\sim 2 \times 10^{12}$
$E(0^+_{gs})$ (MeV)	-370.630	-372.717

Discrete Non-Orthogonal Shell Model (DNO-SM)

- Broeckhove-Deumens Theorem: Z. Phys. A**292**, 243 (1979)

  Given a separable Hilbert space $\mathscr{H}$ spanned by a continuous family of states $\Gamma = \{\psi(\alpha)|\alpha \in \mathbb{R}\}$, there exists a countable subset $\Gamma_0 = \{\phi(\alpha_i)|i \in \mathbb{N}\} \subset \Gamma$ with the property $\mathscr{H} = \overline{\text{span}\Gamma_0}$, i.e. Γ_0 is a skew or non-orthogonal basis in $\mathscr{H}$.

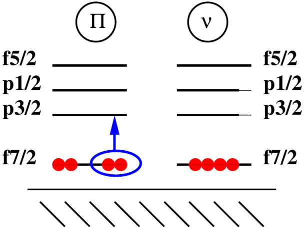

$$\psi = c_1\phi_1 + c_2\phi_2 + \cdots + c_3\phi_3 + \ldots$$

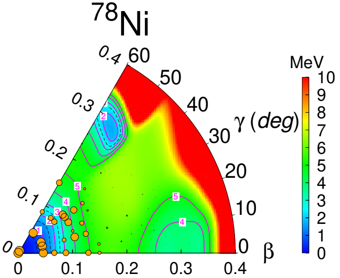

PFSDG-U effective interaction

^{78}Ni	DNO-SM(β,γ)	SM (10p-10h)
dimension	81	$\sim 2 \times 10^{12}$
$E(0^+_{gs})$ (MeV)	-370.630	-372.717

Discrete Non-Orthogonal Shell Model (DNO-SM)

- Broeckhove-Deumens Theorem: Z. Phys. A**292**, 243 (1979)

  Given a separable Hilbert space $\mathscr{H}$ spanned by a continuous family of states $\Gamma = \{\psi(\alpha) | \alpha \in \mathbb{R}\}$, there exists a countable subset $\Gamma_0 = \{\phi(\alpha_i) | i \in \mathbb{N}\} \subset \Gamma$ with the property $\mathscr{H} = \overline{\text{span}\Gamma_0}$, i.e. Γ_0 is a skew or non-orthogonal basis in $\mathscr{H}$.

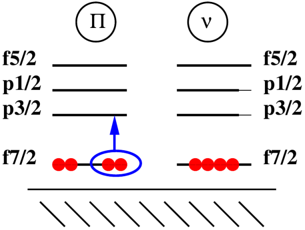

$$\Rightarrow \quad \psi = c_1\phi_1 + c_2\phi_2 + \cdots + c_3\phi_3 + \ldots$$

^{48}Cr with KB3 effective interaction

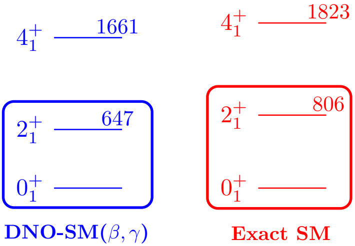

◇ Several questions

- Ground state underbinding energy ?
- Incorporation of correlations ?
- Numerical proof of Broeckhove-Deumens Theorem ?

1. Projection After Variation : DNO-SM(PAV)

◇ Hill-Wheeler-Griffin generator coordinate method:

- $\langle J_z \rangle$, $(q_{20}, q_{22}) \equiv (\beta, \gamma)$ (cranking, axial and triaxial)
- Contribution of $q = (\beta, \gamma)$ in the correlated state J_α
- Rotational symmetry restoration

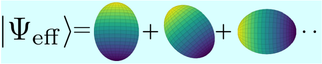

$$P_\alpha^{(J)}(q) = \sum_K |M_\alpha^{(J)}(q,K)|^2$$

(D.D. Dao and F. Nowacki, PRC 105, 054314 (2022))

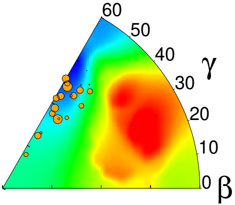

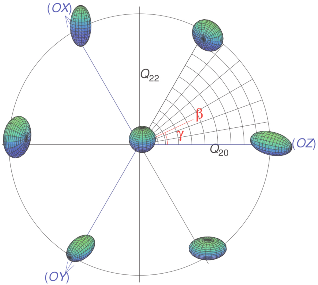

◇ *K*-mixing contents of the wave functions in the instrinsic frame

- K: Projection of total angular momentum J onto the intrinsic axis
- Contribution of K-components in the correlated state J_α

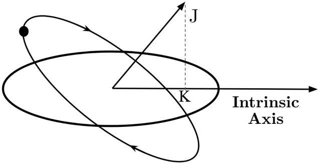

$$P_\alpha^{(J)}(K) = \sum_q |M_\alpha^{(J)}(q,K)|^2$$

2. Variation After Projection : DNO-SM(VAP)

◇ Trial symmetry-projected Slater determinants:

$$\mathcal{H}_{\text{eff}}|\Psi_\alpha^{JM}\rangle = E_\alpha^{(J)}|\Psi_\alpha^{JM}\rangle \Longrightarrow \delta\frac{\langle\Psi_\alpha^{JM}|\mathcal{H}_{\text{eff}}|\Psi_\alpha^{JM}\rangle}{\langle\Psi_\alpha^{JM}|\Psi_\alpha^{JM}\rangle} = 0, \quad |\Psi_\alpha^{JM}\rangle = \sum_{q,K} f_\alpha^{(J)}(q,K)\,\mathcal{P}_{MK}^{J}|\Phi(q)\rangle$$

Double variation AFTER Angular Momentum Projection: Mixing coefficient Slater state

◇ DNO-SM(VAP)

- $q = 1, 2, 3, \ldots$
- $J_\alpha = 0_1, \ldots$
- Best energy-favoring Slater states

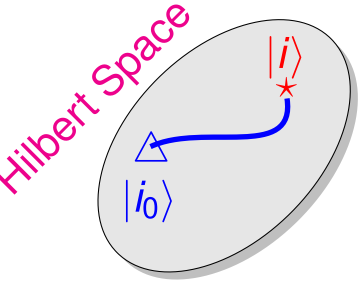

◇ Energy minimization:

$$|\Phi\rangle = e^{\sum_{ij} Z_{ij} c_i^\dagger c_j}|\Phi_0\rangle$$

⇓

$$\frac{\partial E_\alpha^{(J)}}{\partial Z}, \; |\Phi\rangle = |\Phi_0\rangle + \eta\frac{\partial E_\alpha^{(J)}}{\partial Z}$$

⇓

$$E_\alpha^{(J)}, \; |\Psi_\alpha^{JM}\rangle$$

2. Variation After Projection : DNO-SM(VAP)

◇ Trial symmetry-projected Slater determinants:

$$\mathcal{H}_{\mathrm{eff}}|\Psi^{JM}_{\alpha}\rangle = E^{(J)}_{\alpha}|\Psi^{JM}_{\alpha}\rangle \Longrightarrow \delta\frac{\langle\Psi^{JM}_{\alpha}|\mathcal{H}_{\mathrm{eff}}|\Psi^{JM}_{\alpha}\rangle}{\langle\Psi^{JM}_{\alpha}|\Psi^{JM}_{\alpha}\rangle} = 0, \quad |\Psi^{JM}_{\alpha}\rangle = \sum_{q,K} f^{(J)}_{\alpha}(q,K)\,\mathcal{P}^{J}_{MK}\,|\Phi(q)\rangle$$

Double variation AFTER Angular Momentum Projection: Mixing coefficient Slater state

◇ DNO-SM(VAP)

- $q = 1, 2, 3, \ldots$
- $J_{\alpha} = 0_1, \ldots$
- Best energy-favoring Slater states

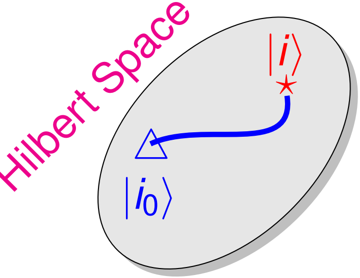

◇ DNO-SM(PAV): (β, γ) + $NpNh$

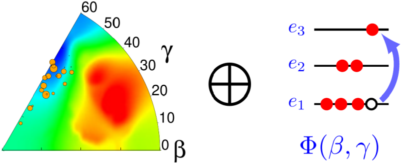

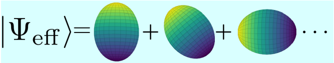

(D.D. Dao and F. Nowacki, in preparation (2024))

Numerical realization of Broeckhove-Deumens Theorem :

USDB effective interaction[a] with non-orthogonal Slater Determinants

([a] B.A. Brown, W. A. Richter, PRC74, 034315 (2006))

	DNO-SM(PAV)		DNO-SM(VAP)	Exact SM
	(β,γ)	(β,γ)+*NpNh*		
^{20}Ne	−40.35736	−40.47233	−40.47231	−40.47233
	7	51	3	640
^{24}Mg	−86.73278	−87.10428	−87.10405	−87.10445
	16	975	16	28503
^{28}Si	−135.21742	−135.85891	−135.86003	−135.86073
	27	4255	45	93710
^{26}Al	–	–	−105.74901	−105.74934
	–	–	22	26914

◇ DN

- q =
- J_α
- Be

Hilber

Backbending in ^{48}Cr with KB3 interaction

	DNO-SM(β, γ)	DNO-SM(VAP)	Exact SM
dimension	22	40	1 963 461
$E(0^+_{gs})$ (MeV)	-31.873	-32.950	-32.953

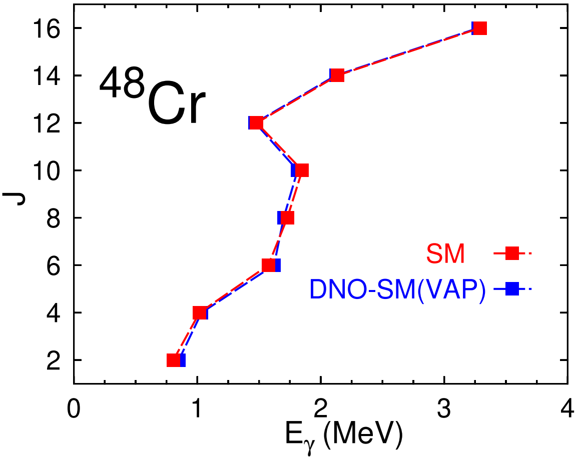

Matching the shell-model solution in ^{78}Ni

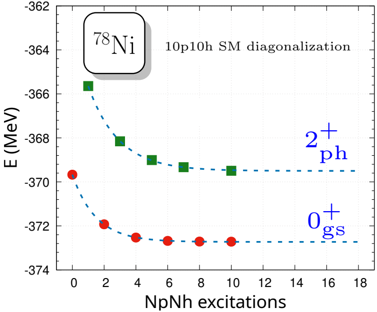

PFSDG-U effective interaction

Ground State Energy in MeV

(β,γ)	VAP	SM (10p-10h)
81	19	$\sim 2 \times 10^{12}$
−370.630	−372.733	−372.717

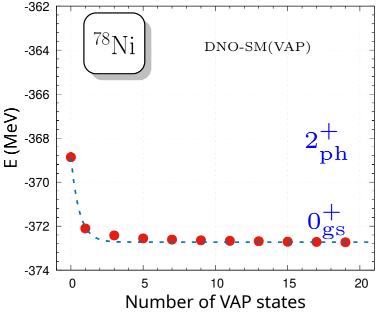

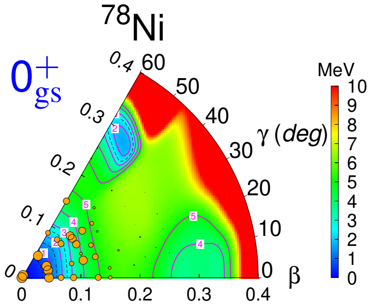

Strong mixing in ^{86}Mo around the N=Z line

ZBM3 effective interaction

Ground State Energy in MeV

DNO-SM(β, γ)	DNO-SM(VAP)	SM (10p-10h)
104	44	$\sim 10^{11}$
-388.383	-391.688	-391.453

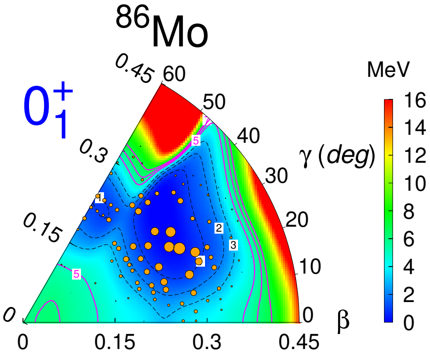

$\Longrightarrow$ See Frédéric Talk

Applications to superheavy nuclei

Kuo-Herling interaction:

- $^{208}_{82}Pb_{126}$ core, realistic TBMEs
- $82 \leq Z \leq 126$ shells for proton and $126 \leq N \leq 184$ for neutrons
- monopole corrections (3N force)

*E. Caurier and F. Nowacki, PRL **87** (2001),072511*

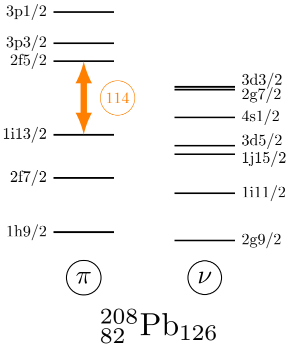

Calculations: NATHAN & CARINA codes

◇ Diagonalization within the seniority scheme along the chains of $N = 126$ and $N = 184$

◇ Variation After Projection calculations: $^{253,254,255}Es$, $^{249,251,253}Cf$, $^{253,254}No$, ^{256}Fm

◇ Comparison of spectra and electromagnetic moments

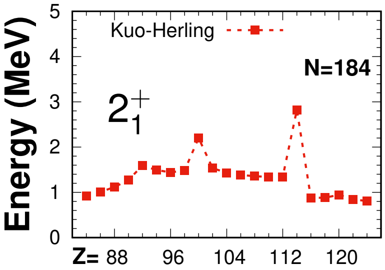

Applications to superheavy nuclei : Yrast systematics

First complete description of low-lying spectroscopy in ^{254}No

Duy Duc Dao[1] and Frédéric Nowacki[1]

[1] *Université de Strasbourg, CNRS, IPHC UMR7178, 23 rue du Loess, F-67000 Strasbourg, France*

arXiv:2409.08210

- ◇ Systematic comparison of Yrast bands

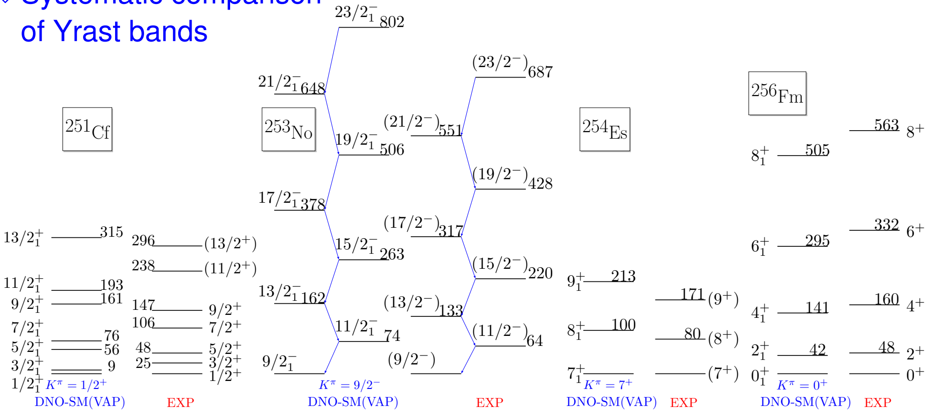

Applications to superheavy nuclei : Electromagnetic moments

First complete description of low-lying spectroscopy in ^{254}No

Duy Duc Dao[1] and Frédéric Nowacki[1]

[1] Université de Strasbourg, CNRS, IPHC UMR7178, 23 rue du Loess, F-67000 Strasbourg, France

arXiv:2409.08210

◇ Comparison of magnetic and quadrupole moments

Effective charges: e_p = 1.72, e_n = 0.75

J^{π}_{gs}		E (MeV)		$\mu(\mu_N)$			Q_s (eb)		
		PHF	VAP	PHF	VAP	EXP	PHF	VAP	EXP
^{253}No	$9/2^-$	−241.818	−242.816	+0.591	−0.493	−0.527(33)(75)	−3.5	+7.2	+5.9(1.4)(0.9)
^{253}Cf	$7/2^+$	−253.402	−253.818	−0.677	−0.556	−0.731(35)	+5.77	+5.78	+5.53(51)
^{251}Cf	$1/2^+$	−241.321	−241.724	−0.727	−0.610	−0.571(24)	-	-	-
^{249}Cf	$9/2^-$	−229.021	−229.381	−0.480	−0.461	−0.395(17)	+6.62	+6.63	+6.27(33)
^{255}Es	$7/2^+$	−263.512	−264.695	−1.10	+3.94	+4.14(10)	+6.0	+5.8	+5.1(1.7)
^{254}Es	7^+	−257.492	−258.441	+0.778	+3.36	+3.42(7)	+1.8	+8.4	+9.6(1.2)
^{253}Es	$7/2^+$	−251.837	−252.280	+3.63	+3.93	+4.10(7)	+5.87	+5.9	+6.7(8)
^{256}Fm	0^+	−268.999	−269.717	+0.87	+0.89	-	−3.57	−3.60	-
^{254}No	0^+	−249.568	−250.187	+0.87	+0.91	-	−3.78	−3.75	-

Applications to superheavy nuclei : Electromagnetic moments

First complete description of low-lying spectroscopy in ^{254}No

Duy Duc Dao[1] and Frédéric Nowacki[1]

[1] *Université de Strasbourg, CNRS, IPHC UMR7178, 23 rue du Loess, F-67000 Strasbourg, France*

arXiv:2409.08210

◇ Comparison of magnetic and quadrupole moments

Effective charges: e_p = 1.72, e_n = 0.75

	J^{π}_{gs}	E (MeV)		$\mu(\mu_N)$			Q_s (eb)		
		PHF	VAP	PHF	VAP	EXP	PHF	VAP	EXP
^{253}No	9/2$^-$	−241.818	−242.816	+0.591	−0.493	−0.527(33)(75)	−3.5	+7.2	+5.9(1.4)(0.9)
^{253}Cf	7/2$^+$	−253.402	−253.818	−0.677	−0.556	−0.731(35)	+5.77	+5.78	+5.53(51)
^{251}Cf	1/2$^+$	−241.321	−241.724	−0.727	−0.610	−0.571(24)	-	-	-
^{249}Cf	9/2$^-$	−229.021	−229.381	−0.480	−0.461	−0.395(17)	+6.62	+6.63	+6.27(33)
^{255}Es	7/2$^+$	−263.512	−264.695	−1.10	+3.94	+4.14(10)	+6.0	+5.8	+5.1(1.7)
^{254}Es	7$^+$	−257.492	−258.441	+0.778	+3.36	+3.42(7)	+1.8	+8.4	+9.6(1.2)
^{253}Es	7/2$^+$	−251.837	−252.280	+3.63	+3.93	+4.10(7)	+5.87	+5.9	+6.7(8)
^{256}Fm	0$^+$	−268.999	−269.717	+0.87	+0.89	-	−3.57	−3.60	-
^{254}No	0$^+$	−249.568	−250.187	+0.87	+0.91	-	−3.78	−3.75	-

Applications to superheavy nuclei : Electromagnetic moments

First complete description of low-lying spectroscopy in ^{254}No

Duy Duc Dao[1] and Frédéric Nowacki[1]
[1] *Université de Strasbourg, CNRS, IPHC UMR7178, 23 rue du Loess, F-67000 Strasbourg, France*

arXiv:2409.08210

◇ Comparison of magnetic and quadrupole moments

Effective charges: e_p = 1.72, e_n = 0.75

^{253}No	PHF	VAP	EXP
$J^\pi = 9/2^-$	$+0.591$	-0.493	$-0.527(33)(75)$
$K = 9/2$	100.0%	99.6%	
$K = 7/2$	0.0 %	0.4 %	

- K-mixing is necessary to reproduce the magnetic moment.

Applications to superheavy nuclei : ^{254}No

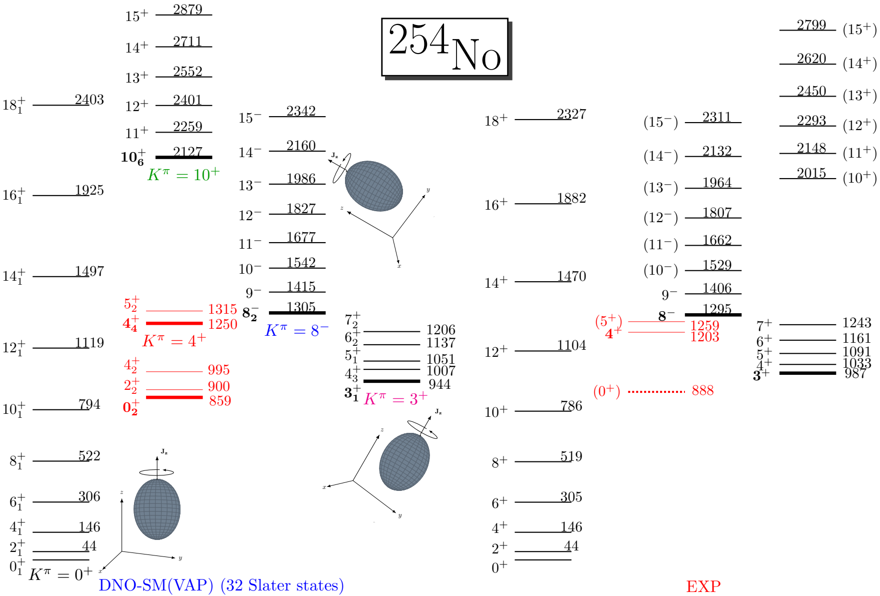

Applications to superheavy nuclei : ^{254}No

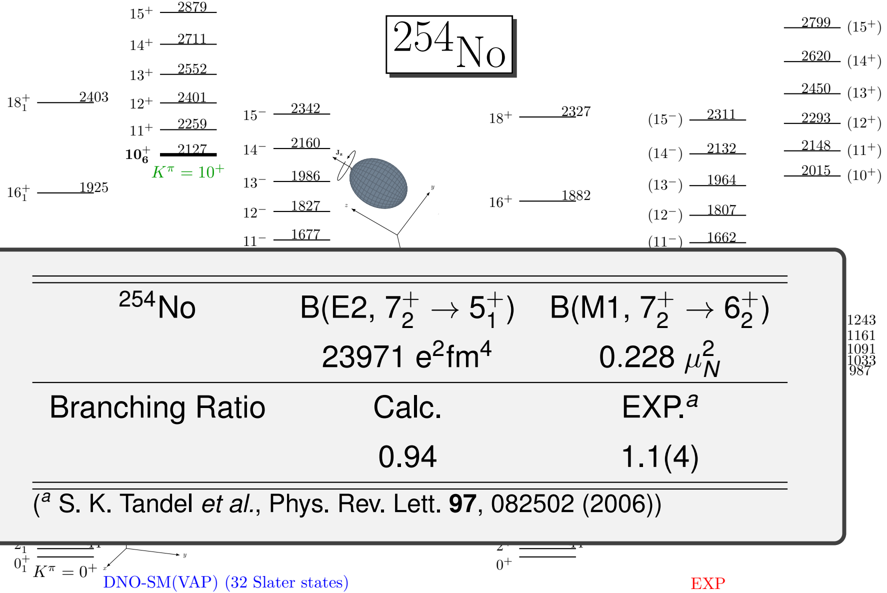

^{254}No	$B(E2, 7_2^+ \rightarrow 5_1^+)$	$B(M1, 7_2^+ \rightarrow 6_2^+)$
	23971 e^2fm^4	0.228 μ_N^2
Branching Ratio	Calc.	EXP.[a]
	0.94	1.1(4)

([a] S. K. Tandel *et al.*, Phys. Rev. Lett. **97**, 082502 (2006))

Applications to superheavy nuclei : Pairing correlations in ^{254}No

First complete description of low-lying spectroscopy in ^{254}No

Duy Duc Dao[1] and Frédéric Nowacki[1]

[1] *Université de Strasbourg, CNRS, IPHC UMR7178, 23 rue du Loess, F-67000 Strasbourg, France*

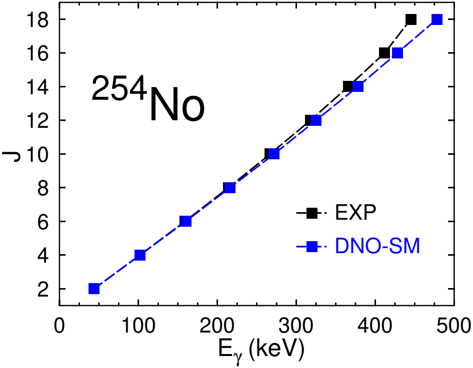

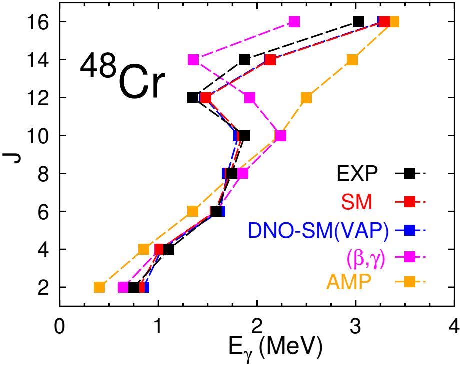

Applications to superheavy nuclei : Pairing correlations in ^{254}No

First complete description of low-lying spectroscopy in ^{254}No

Duy Duc Dao[1] and Frédéric Nowacki[1]
[1] *Université de Strasbourg, CNRS, IPHC UMR7178, 23 rue du Loess, F-67000 Strasbourg, France*

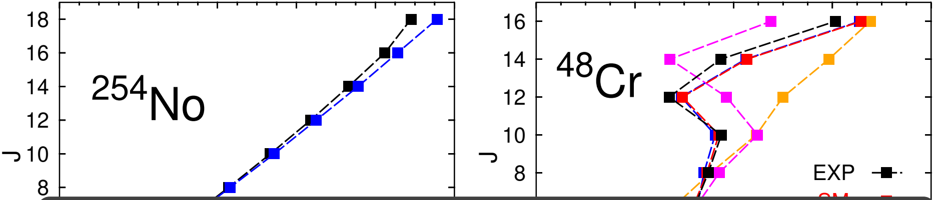

- Experimental spectrum shows a perfect rotational band behaviour $J(J+1)$.
- Quadrupole regime strongly dominates, pairing correlations are negligible.

Conclusions

- The DNO-SM exactly matches the Shell Model solutions.
- Broeckhove-Deumens Theorem is proved numerically in various physics regimes.
- Pairing correlations are perfectly captured by non-orthogonal Slater Determinants without using Hartree-Fock-Bogoliubov wavefunctions nor breaking the particle numbers.
- First shell-model calculations for superheavy nuclei in the ^{254}No region show an excellent agreement with experiments.
- Complete description of both the rotational band and various excited K bands and isomeric states in ^{254}No.

THANK YOU FOR YOUR ATTENTION !

BACKUP

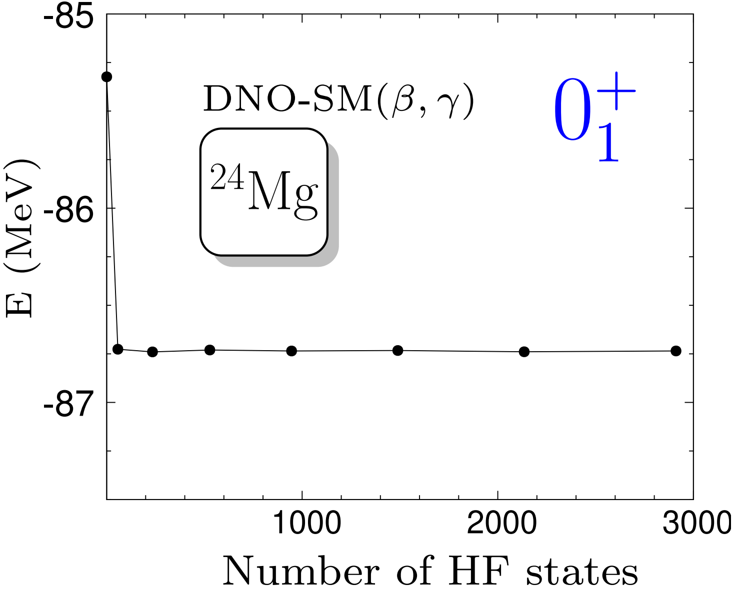

-85
-86
-87
E (MeV)
DNO-SM(β,γ)
^{24}Mg
0_1^+
1000
2000
3000
Number of HF states

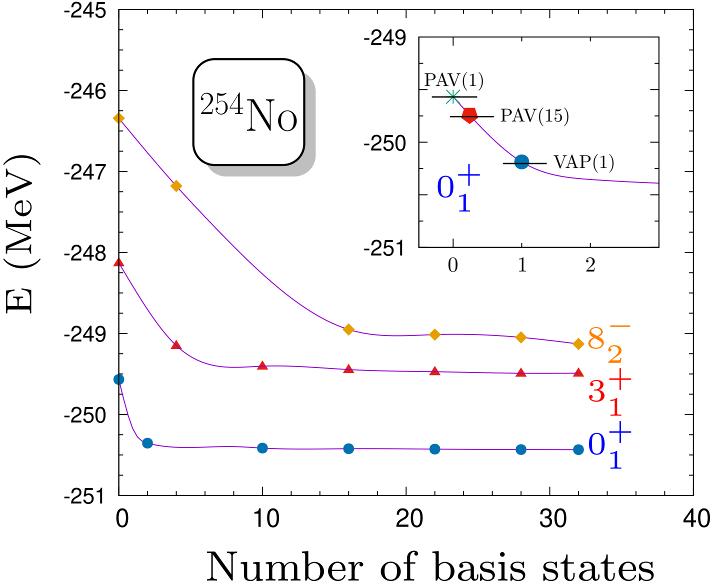

-245
-246
-247
-248
-249
-250
-251
0
10
20
30
40
E (MeV)
Number of basis states
254No
8 2 −
3 1 +
0 1 +
-249
-250
-251
0
1
2
PAV(1)
PAV(15)
VAP(1)
0 1 +

Proton orbits	$0h_{9/2}$	$0i_{13/2}$	$1f_{7/2}$	$1f_{5/2}$	$2p_{3/2}$	$2p_{1/2}$	
0_1^+	6.03	7.75	3.43	1.49	0.77	0.52	
0_2^+	7.08	7.91	3.23	0.89	0.69	0.21	
$3_1^+(K=3)$	6.47	7.98	3.34	1.15	0.72	0.34	
$4_4^+(K=4)$	6.50	7.83	3.41	1.18	0.72	0.36	
$8_2^-(K=8)$	6.48	7.90	3.36	1.19	0.70	0.37	
$10_6^+(K=10)$	6.55	7.03	3.48	1.56	0.79	0.58	
Neutron orbits	$0i_{11/2}$	$0j_{15/2}$	$1g_{9/2}$	$1g_{7/2}$	$2d_{5/2}$	$2d_{3/2}$	$3s_{1/2}$
0_1^+	7.30	9.91	5.43	1.00	1.09	0.84	0.43
0_2^+	7.36	9.95	5.45	0.96	1.05	0.80	0.42
$3_1^+(K=3)$	7.32	9.94	5.46	0.97	1.07	0.81	0.42
$4_4^+(K=4)$	7.34	9.79	5.48	1.03	1.11	0.81	0.44
$8_2^-(K=8)$	7.42	9.00	6.30	0.98	1.06	0.81	0.43
$10_6^+(K=10)$	7.23	8.89	5.72	1.40	1.34	0.97	0.45

$J_i^\pi \rightarrow$	J_f^π	$B(E2)$ ($e^2.fm^4$)	$B(M1)$ (μ_N^2)
$2_1^+ \rightarrow$	0_1^+	28666	-
$4_1^+ \rightarrow$	2_1^+	41021	-
$0_2^+ \rightarrow$	2_1^+	98.236	-
$2_2^+ \rightarrow$	0_2^+	25327	-
	4_1^+	60.738	-
	2_1^+	25.227	3.980×10^{-6}
$3_1^+ \rightarrow$	2_2^+	2.5959×10^{-2}	8.020×10^{-6}
	4_1^+	2.7359×10^{-4}	2.957×10^{-7}
	2_1^+	9.6147×10^{-4}	6.050×10^{-6}
$4_2^+ \rightarrow$	2_2^+	36147	-
	3_1^+	5.4204×10^{-1}	4.200×10^{-7}
	4_1^+	23.783	8.360×10^{-6}
	2_1^+	18.569	-
$4_3^+ \rightarrow$	3_1^+	45803	1.3852×10^{-1}
	6_1^+	6.3712×10^{-4}	-
	4_1^+	6.5482×10^{-3}	3.634×10^{-5}
	2_1^+	8.2100×10^{-6}	-
$4_4^+ \rightarrow$	3_1^+	1.1354×10^{3}	1.977×10^{-3}
	4_3^+	9.6847×10^{2}	1.737×10^{-2}
	2_2^+	4.438×10^{-4}	-
	2_1^+	1.398×10^{-4}	-